the plant journal

SEB SOCIETY FOR EXPERIMENTAL BIOLOGY

The Plant Journal (2009) **59**, 426–436 doi: 10.1111/j.1365-313X.2009.03874.x

Arabidopsis plant homeodomain finger proteins operate downstream of auxin accumulation in specifying the vasculature and primary root meristem

Carole L. Thomas[1], Dominik Schmidt[1,†], Emmanuelle M. Bayer[2], Rene Dreos[1] and Andrew J. Maule[1,*]

[1]*John Innes Centre, Norwich Research Park, Colney, Norwich NR4 7UH, UK, and*

[2]*Institute of Plant Sciences, University of Bern, Altenbergrain 21, CH-3013 Bern, Switzerland*

Received 23 December 2008; revised 4 March 2009; accepted 13 March 2009; published online 23 April 2009.

[*]For correspondence (fax +44 1603 450045; e-mail andy.maule@bbsrc.ac.uk).

[†]Present address: Qiagen GmbH, Qiagenstrasse 1, D-40724 Hilden, Germany.

SUMMARY

In *Arabidopsis thaliana*, auxin is a key regulator of tissue patterning in the developing embryo. We have identified a group of proteins that act downstream of auxin accumulation in auxin-mediated root and vascular development in the embryo. Combined mutations in *OBERON1* (*OBE1*) and *OBERON2* (*OBE2*) give rise to *obe1 obe2* double mutant seedlings that closely phenocopy the *monopteros* (*mp*) mutant phenotype, with an absence of roots and defective development of the vasculature. We show that, in contrast to the situation in *mp* mutants, *obe1 obe2* double mutant embryos show auxin maxima at the root pole and in the provascular region, and that the SCF^{TIR1} pathway, which translates auxin accumulation into transcriptional activation of auxin-responsive genes, remains intact. Although we focus on the impact of *obe* mutations on aspects of embryo development, the effect of such mutations on a broad range of auxin-related gene expression and the tissue expression patterns of *OBE* genes in seedlings suggest that OBE proteins have a wider role to play in growth and development. We suggest that OBE1 and OBE2 most likely control the transcription of genes required for auxin responses through the action of their PHD finger domains.

Keywords: Arabidopsis, auxin, plant homeodomain finger protein, root meristem, vascular development.

INTRODUCTION

Early plant embryo development establishes apical–basal polarity (reviewed by Jenik *et al.*, 2007). Communication between these poles is achieved via the vascular network, the primary elements of which are specified during early embryo development. Hormone signalling plays a key role in defining the framework of the body pattern, and central to the formation of the root and the vascular network is the hormone auxin (reviewed by De Smet and Jürgens, 2007; Galweiler *et al.*, 1998; Berleth *et al.*, 2000; Scarpella *et al.*, 2006).

Auxin is effective as a signalling molecule through formation of local gradients. Polar auxin transport is mediated by families of auxin influx carriers (e.g. AUX1) and efflux proteins called PINs (Yang *et al.*, 2006; Wisniewska *et al.*, 2006; reviewed by Blakeslee *et al.*, 2005; Kramer and Bennett, 2006). The channelling of auxin by PIN proteins into local dynamic maxima is referred to as 'canalization'. These maxima activate downstream transcriptional networks and cell-type specification (Benkova *et al.*, 2003; reviewed by Leyser, 2006). Since Aux/IAA proteins act as negative regulators by complexing with auxin-responsive transcription factors (ARFs), transcriptional activation depends upon dissociation of the protein complexes. Hence, SCF^{TIR1}- and proteosome-mediated degradation of Aux/IAA proteins leads to activation of auxin-responsive genes (Gray *et al.*, 2001; Dharmasiri *et al.*, 2005; Tan *et al.*, 2007). In the roles of negative regulator and transcriptional activator, the factors Aux/IAA12 or BODENLOS (BDL) and ARF5 or MONOPTEROS (MP), respectively, are important in specifying the root apical meristem and the vasculature (Berleth and Jürgens, 1993; Hardtke and Berleth, 1998; Hamann *et al.*, 1999, 2002; Weijers *et al.*, 2005).

After early divisions of the Arabidopsis embryo, auxin is concentrated in the apical tissues through the action of PIN7. In late globular and heart stage embryos, PIN1 mediates upward transport of auxin in the epidermis to define the position of the cotyledonary primordia and downward canalization through the centre of the embryo to concentrate auxin in the uppermost basal cell (hypophysis). After an

asymmetric division, this cell becomes the progenitor of the quiescent centre (QC) and columella cells of the root cap. High auxin concentrations in central cells of the embryo cause them to elongate and differentiate into procambial cells that map out the vascular connections between the root and the emerging cotyledons (Friml *et al.*, 2003; Benkova *et al.*, 2003; Weijers *et al.*, 2006; reviewed by Weijers and Jürgens, 2005).

We are investigating the function of two proteins identified from a yeast two-hybrid screen for interactors with a potyvirus protein, VPg. We called these proteins potyvirus VPg-interacting proteins (PVIP1 and 2) (Dunoyer *et al.*, 2004). These proteins each contain a plant homeodomain (PHD) as their only recognizable functional domain, and have the potential to regulate gene expression through histone modifications (Martin *et al.*, 2006; Peňa *et al.*, 2006; Ramon-Maiques *et al.*, 2007; reviewed by Cosgrove, 2006). PVIP2 and PVIP1 correspond to OBERON1 (OBE1) and OBERON2 (OBE2), respectively, which have been described (Saiga *et al.*, 2008) as having redundant functions in the establishment and/or maintenance of the shoot and root apical meristems.

Here we describe detailed phenotypes for the *obe1 obe2* double mutant in the context of auxin as a signal for root and vascular specification, and show that OBE1 and OBE2 operate downstream of auxin canalization in the early stages of embryo development. We show that, in *obe1 obe2* mutants, defects in the basal embryonic tissues result in a failure in root growth related to loss of auxin signalling. In common with examples of other auxin-signalling mutants, we also show that *obe1 obe2* mutants are defective in vascular patterning. By combining *obe1 obe2* double mutants with known mutants in auxin signalling, by following the formation of auxin maxima in the developing embryo, and by assessing the functionality of the SCF^{TIR1} pathway, we also show that OBE proteins control these processes at a point downstream of auxin accumulation and sensing. The impacts of OBE functions on root and shoot meristems and on vascular patterning suggest that OBE proteins act as central regulators in auxin-mediated control of development.

RESULTS

OBE1 and OBE2 are required for development of the basal pole

To investigate the biological roles of OBE1 and OBE2, we used a T-DNA insertion mutant line for *OBE1* (SALK_075710; *obe1-1*) (Saiga *et al.*, 2008), and a TILLING mutant line for *OBE2* with a G → A transition in the PHD finger region that generated a premature stop codon (called *obe2-2*). Neither mutant line showed a phenotype that was different from that of wild-type plants.

The phenotype of the *obe1-1 obe2-2* double mutant was identical to that of the previously described *obe1-1 obe2-1* double mutant (Saiga *et al.*, 2008). This included the absence of a primary root and variable numbers of cotyledons, occasionally either lobed or fused, and defective development of the first pair of leaves (Figure 1a–d,k). Despite the absence of a primary root, mutant seedlings still showed formation of root hairs at the base of the hypocotyl, indicating that root tissues above the basal pole were correctly specified (Figure 1a,b). In addition, *obe1-1 obe2-2* double mutants showed severe restriction of the vasculature in hypocotyl tissues (Figure 1e,f) and a disrupted pattern in cotyledons (Figure 1g,h).

The *obe1-1 obe2-2* mutant phenotype was similar to that of severe mutants of *MP* and *BDL*. *MP* encodes a transcription factor that activates genes that are positively regulated by auxin. Direct binding of BDL to MP blocks MP function, an inhibition that is relieved by auxin-mediated degradation of BDL. *bdl* is an incompletely dominant mutation encoding a stabilized variant of the BDL protein that fails to dissociate from the MP/BDL ARF-Aux/IAA complex in the presence of auxin (Hamann *et al.*, 2002; Weijers *et al.*, 2006). Mutants *mpG12*, *bdl* and *obe1-1 obe2-2* did not develop roots but were subtly different with regard to the formation of vestigial root tissues (Figure 1k,m). Also, both *mpG12* and *bdl* show defects in vascular patterning (Figure 1i,j), although these were more severe than vascular phenotypes in the *obe1-1 obe2-2* double mutants (Figure 1h,j). These observations suggest that OBE, MP and BDL proteins affect similar developmental processes.

The absence of primary root growth but retention of features such as root hairs, associated with the root body, indicated a defect in development of the basal pole in *obe1-1 obe2-2* double mutant embryos. This prompted a detailed examination of defects in early embryo development. The earliest defects in embryo development were visible in globular stage embryos when asymmetric division of the hypophysis failed to occur. Instead, mutant embryos showed chaotic divisions of the hypophysis (data not shown; Saiga *et al.*, 2008). Although, in many cases, divisions of outer apical cells (progenitors of the root epidermis and cortex) remained unaffected, mutant embryos also showed disorganization of incipient procambial cells (Figure 2b,d). In later embryos, subsequent divisions gave rise to grossly disorganized tissues with no discernible root or vascular patterning. These data indicate that a first effect of the *obe1-1 obe2-2* double mutation is failure of the hypophysis to correctly specify the QC, and that the impacts of OBE activity extend into apical tissues and to development of the root and hypocotyl vasculature.

To confirm that the *obe1-1* insertional mutation and the *obe2-2* TILLING mutation were the cause of the seedling phenotypes, *obe1-1/obe1-1 OBE2/obe2-2* and *OBE1/obe1-1 obe2-2/obe2-2* plants were transformed with constructs carrying *OBE1p:OBE1* or *OBE2p:OBE2* Arabidopsis genomic

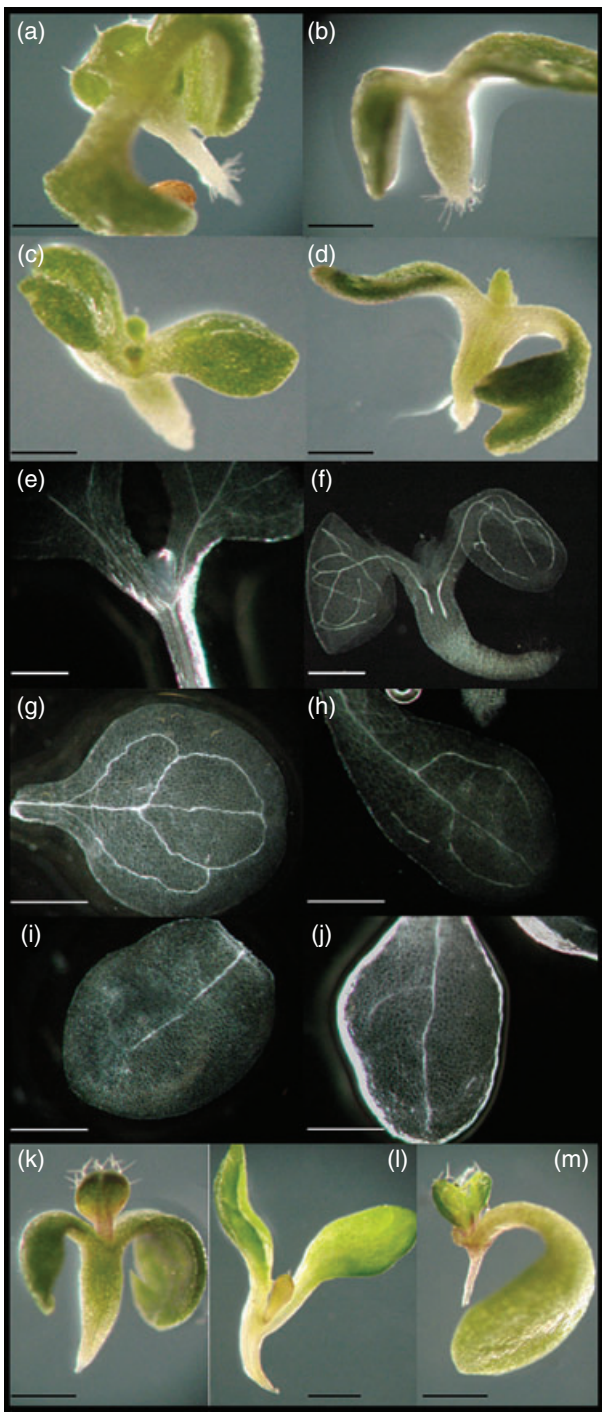

Figure 1. Phenotype of *obe1-1 obe2-2* mutant seedlings.
(a–d) 'Rootless' phenotypes of 7-day-old seedlings of the *obe1-1 obe2-2* mutant, and a range of cotyledon morphologies including triple cotyledons (a) and fused (c) or lobed (d) cotyledons.
(e–j) The vascular network was defective in 9-day-old seedlings of *obe1-1 obe2-2* (f, h), *mpG12* (i) and *bdl* (j) mutants compared to Arabidopsis Col-0 (e, g).
(k–m) Twelve-day-old seedlings of *obe1-1 obe2-2* (k), *bdl* (l) and *mpG12* (m) show subtly different root phenotypes.
Scale bars = 0.5 mm.

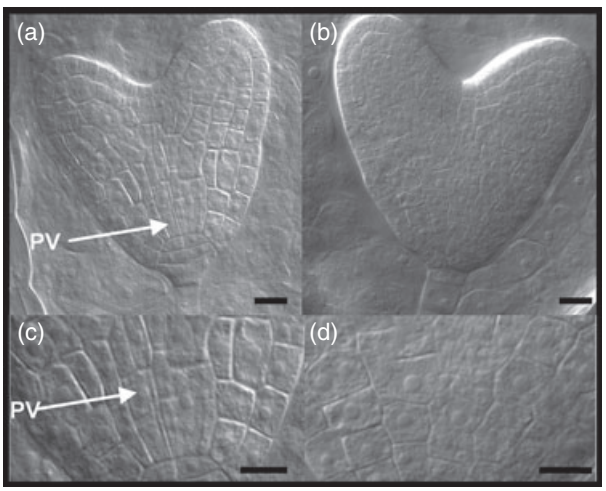

Figure 2. Embryonic phenotype of *obe1-1 obe2-2* mutants.
(a–d) Embryos of Arabidopsis Col-0 (a, c) and *obe1-1 obe2-2* (b, d) at the developmental heart stage showing disorganization of the provasculature in the mutant. PV, provasculature. Scale bars = 10 μm.

fragments, respectively, and rescued double mutant transformants were identified genotypically. In each case, multiple lines with double mutant genotypes and wild-type phenotype demonstrated complementation of the obe1-1 and obe2-2 alleles. Similar data were obtained using the *AtRPS5A* embryo-expressed promoter (Weijers *et al.*, 2001). In contrast, no rescue of mutant plants occurred when the binary vector contained the CaMV 35S promoter controlling expression of *OBE2* cDNA. The CaMV 35S promoter is known not to be functional in embryonic tissues (Sunilkumar *et al.*, 2002), confirming that expression of *OBE1* and *OBE2* during embryogenesis is essential for plant development.

Defects in basal and apical development suggest that *OBE* genes are expressed in both domains, but perhaps particularly in basal tissues and the vasculature. We assessed this by transforming Col-0 plants with constructs expressing GFP fused to a nuclear localization signal (nls) or GFP fused to GUS from the native *OBE* promoters (*OBEp:nlsGFP and OBEp:GFP.GUS*). The promoters were the same as those used for rescuing the *obe1-1 obe2-2* double mutants. Use of nlsGFP as a reporter avoided any misinterpretation of expression patterns due to differences in cell size. Using the *OBEp:nlsGFP* construct, we confirmed (Saiga *et al.*, 2008) that both genes were expressed throughout embryo development (Figure 3). Overlap in expression was expected from the redundant nature of OBE1 and OBE2 functions. Uniform GFP fluorescence was seen in the embryo proper, with only weak expression in the suspensor (data not shown), until the torpedo stage of development when expression was concentrated at the root pole, with weak expression elsewhere. At this stage, expression from *OBE1p* was strongest in the columella and lateral root cap

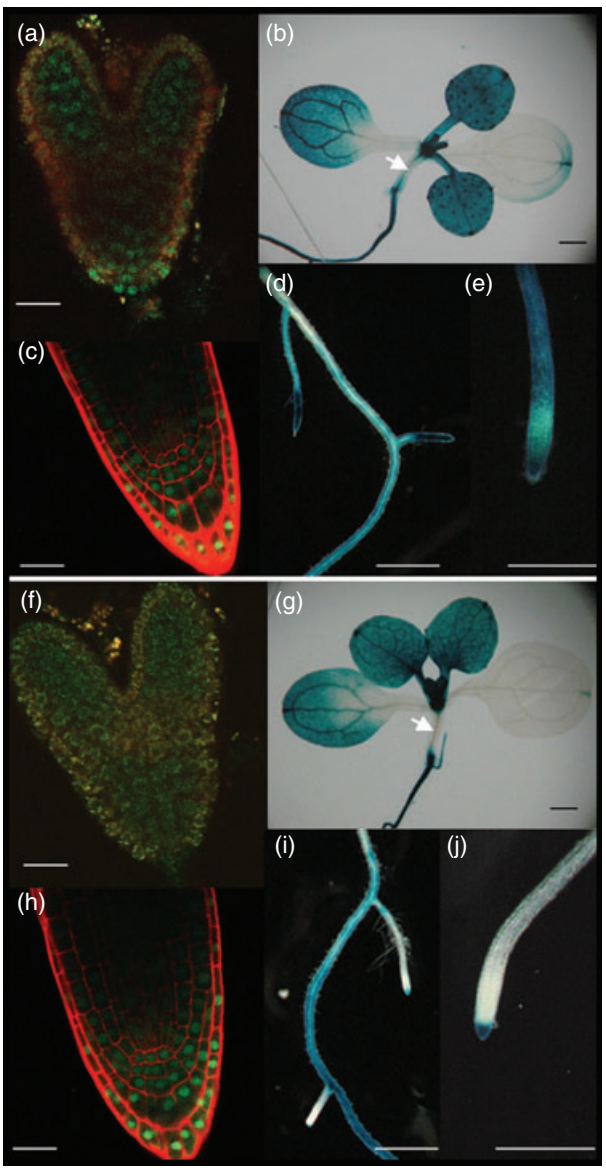

Figure 3. Expression patterns of *OBE1p* and *OBE2p* promoter reporter lines. (a, c, f, h) Reporter *OBE1p:nlsGFP* (a) and *OBE2p:nlsGFP* (f) expression in transgenic Col-0 torpedo stage embryos and in 3-day-old *OBE1p:nlsGFP* (c) and *OBE2p:nlsGFP* (h) transgenic roots, visualized as GFP fluorescence. (b, d, e, g, i, j) Reporter *OBE1p:GFP.GUS* (b, d, e) and *OBE2p:GFP.GUS* (g, i, j) expression in 7-day-old seedlings visualized histochemically as GUS activity. Scale bars = 20 μm (a, c, f, h) or 0.5 mm (b, d, e, g, i, j).

(Figure 3a), whereas expression from *OBE2p* was more uniform (Figure 3f). In seedling roots, *OBE1p* and *OBE2p* expression overlapped completely (Figure 3c,h). The distinction between the activities of the two promoters was more obvious in GUS-stained roots. Although GUS activity was present in mature and fully differentiated young roots (Figure 3d,e,i,j), *OBE1p* expression in young roots (main or lateral) extended from the root cap to the emerging root-hair zone (Figure 3d,e), whereas *OBE2p* expression was restricted to root tips (Figure 3m,n). GUS staining of whole seedlings confirmed *OBE* expression in other plant organs, including the vasculature and ground tissues, although expression in hypocotyls was restricted to the vasculature (Figure 3b,g, arrow). Hence, expression of *OBE1* and *OBE2* overlaps in embryos and seedlings as would be expected for genes with fully redundant functions.

obe1 and obe2 mutations have a broad impact on auxin-related processes

The similarity between the *obe1-1 obe2-2* double mutant seedlings and *mpG12* and *bdl* mutants prompted us to focus our attention on the possibility that OBE function is involved in auxin-directed tissue specification. We approached this in three ways. First, we determined whether *OBE* genes might respond to auxin treatment. Second, we determined whether the *obe1-1 obe2-2* mutation correlates with changes in auxin-related gene expression. Third, we determined whether *obe* mutations showed genetic interactions with centrally involved auxin-related genes, i.e. *MP, BDL* and *PIN1*.

To test the auxin-responsiveness of the *OBE* genes, *OBE1p:GFP.GUS* and *OBE2p:GFP.GUS* plants were grown in the absence and presence of exogenous auxin and stained for GUS activity in the tissues after 8 days. These constructs used promoter fragments that fully complemented *obe1 obe2* mutant phenotypes in seedlings and mature plants (see above). A search of these 1 kb fragments for auxin-responsive transcriptional elements (AREs; TGTCTC), identified only one, 457 bp upstream of the ATG of *OBE2p*. No difference in GUS staining patterns was seen in aerial tissues following auxin treatment. In contrast, in roots, exogenous auxin stimulated expression of both *OBE1* and *OBE2* in the elongation zone (Figure 4). However, the absence of AREs in *OBE1p* and the absence of auxin induction except in root tissue (which shows altered growth and development) meant that increases in *GUS* expression in root tip tissues need not be directly related to auxin induction.

To assess relationships in global gene expression, Arabidopsis ATH1 expression profiles were compared for mutant and wild-type sibling seedlings, and for wild-type and double RNAi lines for *OBE1* and *OBE2* (*obe1i obe2i*) generated by crossing single RNAi lines described previously (*PVIP1i* and *PVIP2i*; Dunoyer *et al.*, 2004). Double RNAi lines were stunted in growth but grew to maturity and seed set, although seed set was poor (data not shown). Although the phenotypic similarity between the *obe1-1 obe2-2* double mutant and mutants in *mp* and *bdl* indicated primary defects in embryonic organ specification, insufficient material for transcript profiling was available from embryos, and seedling tissues were used instead. Roots were removed from wild-type seedlings, and the lower hypocotyl tissue of mutant seedlings was correspondingly wounded. Although our seedling analysis necessarily excluded root-specific

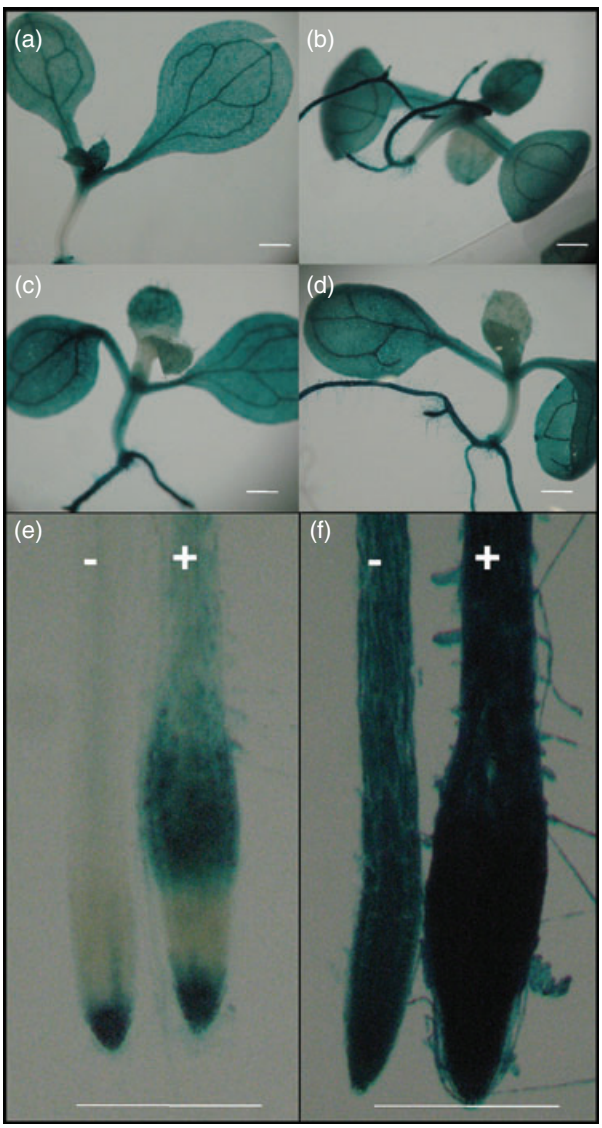

Figure 4. Auxin induction of *OBE1p* and *OBE2p* promoter reporter lines. Eight-day-old *OBE1p:GUS.GFP* (a, b, e) and *OBE2p:GUS.GFP* (c, d, f) transgenic Col-0 were treated with naphthalene acetic acid (b, d) or left untreated (a, c) and stained for GUS activity. (e, f) show a close-up of root tips from *OBE1p* (e) and *OBE2p* (f) reporter lines. Scale bars = 0.5 mm.

gene expression, we hypothesized that the widespread expression of *OBE1* and *OBE2* would have an impact on broad areas of gene expression that would be revealed through analysis of the aerial tissues.

Comparison of *obe1-1 obe2-2* mutant and segregating phenotypic wild-type seedlings, or *obe1i obe2i* seedlings with wild-type seedlings, revealed a large number of significant changes in expression ($P \leq 0.05$; greater than twofold change; Tables S1 and S2). Given the differences in the nature of the biological material, the data from the mutant seedlings and RNAi lines were surprisingly consistent, with 40–45% of induced RNAs in common between the two systems (Figure S1). Analysis of the number of genes with a gene ontology annotation related to auxin signalling showed that this class of genes was significantly over-represented in the changes associated with either the *obe1-1 obe2-2* or *obe1i obe2i* mutant genotypes (Table S3). To validate the microarray data for *obe1-1 obe2-2* mutant seedlings, a number of genes connected with auxin signalling were selected for comparative analysis with segregating wild-type siblings by quantitative RT-PCR (Table S4). For the majority of genes tested, quantitative RT-PCR data confirmed the direction of change seen in microarray data, although the extent of change was much larger in the quantitative RT-PCR analysis. Overall, in the transcript profiling, a number of key auxin-signalling genes showed reduced RNA accumulation, particularly *MP*, *BDL*, *PIN1* and a collection of ARFs. However, down-regulation of auxin-related genes was not universal. Notable was the induction of several important genes in the auxin biosynthesis pathway (Table S5). Although by necessity not focused on changes in gene expression in immature embryos or in developing roots, this analysis showed that, consistent with widespread expression of *OBE* genes in the vegetative tissues, the mutations in *OBE* genes had a broad impact on expression of genes associated with auxin biosynthesis, transport and signalling.

OBE acts close to MP and overlaps with PIN1 and BDL

To assess the genetic interaction between *OBE* genes and *MP*, *BDL* or *PIN1*, triple mutants were generated by crossing the *obe1-1/obe1-1 OBE2/obe2-2* genotype with *mpG12*, *bdl* and *pin1-7* mutants, and the phenotypes of triple mutant genotypes were compared with those of their siblings. *mpG12* and *bdl* mutants alone show a range of phenotypes at the seedling stage (Hardtke and Berleth, 1998; Hamann *et al.*, 1999). The *pin1-7* phenotype is not always apparent at the seedling stage, during which the *pin1* defect is probably compensated for by other members of the PIN family (Friml *et al.*, 2003; Vieten *et al.*, 2005). *obe1-1 obe2-2 pin1-7* seedlings showed the most severe phenotypes (Figure 5c–e), with a range of defects in both basal and apical development. In addition to the absence of a root, shoot meristems were reduced to vestigial structures and cotyledons were completely fused, features that are not typical of either parent mutant. These synergistic interactions indicate overlapping rather than epistatic functions of OBE with respect to PIN1. A similar conclusion was drawn with respect to the *bdl* mutation. Here, triple mutants showed no root, a vestigial hypocotyl, extensively fused cotyledons and no primary leaves (Figure 5g–i), the latter two features being atypical of either parent mutant, again pointing to overlapping functions. A different situation occurred in relation to the triple mutant with *mpG12*. Even though the *mpG12* mutant alone showed as severe a phenotype as *bdl*, the triple *obe1-1 obe2-2 mpG12* mutant showed a range of root and cotyledon

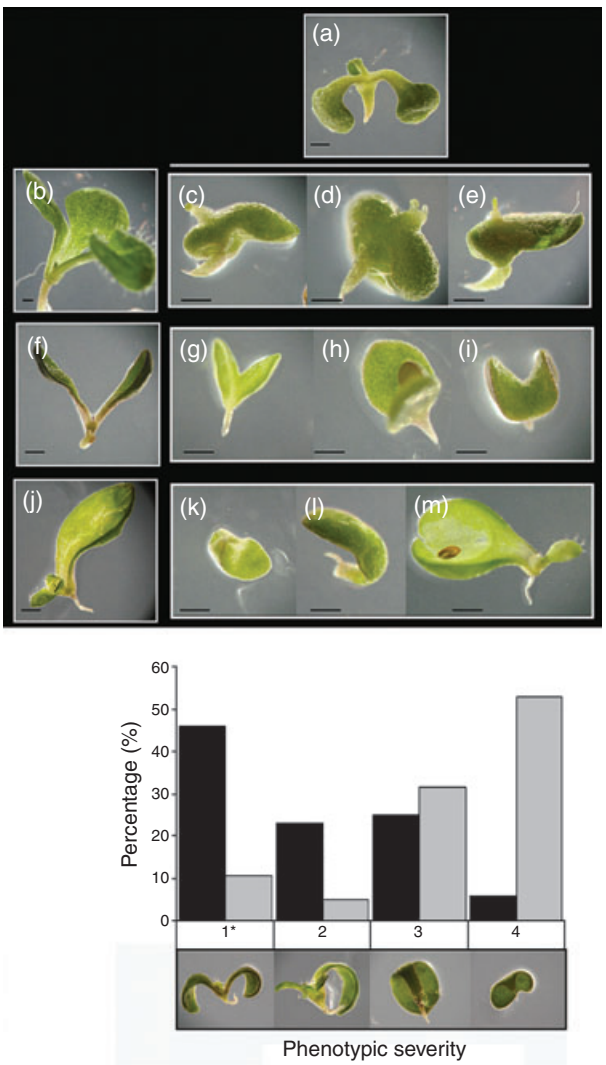

Figure 5. Genetic interaction with *pin1-7*, *bdl* and *mpG12*.
Upper panel: (a–m) phenotypes of 8-day-old seedlings of *obe1-1 obe2-2* (a), *pin1-7* (b), *obe1-1 obe2-2 pin1-7* (c–e), *bdl* (f), *obe1-1 obe2-2 bdl* (g–i), *mpG12* (j) and *obe1-1 obe2-2 mpG12* (k–m). Scale bars = 0.5 mm.
Lower panel: semi-quantitative phenotypic analysis of segregating progeny from a cross between *mpG12* and *obe1-1/OBE1 obe2-2/obe2-2* genotypes. The phenotypes were scored 1–4 as indicated in the illustrations below the graph. Mutants combining *mpG12* with more than one *OBE1* allele (black bars) are compared with the *mpG12 obe1-1 obe2-2* genotype (grey bars).

phenotypes that did not differ significantly from the complete range of phenotypes seen with the *mpG12* mutation alone (Figure 5k–m and lower panel). Notably, the root phenotype was clearly the same as that observed for the *mpG12* mutation rather than the *obe1-1 obe2-2* mutants. The phenotypic severity of triple mutants, and segregating *mpG12* mutants carrying at least one wild-type OBE allele, were scored using an arbitrary scale and compared. Of a total of 187 seedlings, phenotypes of triple mutants (18) were located close to but not exclusively towards the severe end of the range of *mpG12* phenotypes (Figure 5). This is an interaction similar to that observed for the *nph4* mutation (Hardtke *et al.*, 2004) and indicates an epistatic relationship between MP and OBE. With such an epistatic relationship, one possibility was that *OBE* genes could be regulated directly via ARF activity of MP. To test this, *mpG12* seedlings were tested for *OBE1* and *OBE2* expression. RT-PCR analysis showed that *OBE* gene expression was unchanged in *mpG12* mutants (data not shown).

The SCF^{TIR1} pathway is still functional in *obe1-1 obe 2-2* mutants

We have shown that MP is epistatic to OBE, and it has been shown (Saiga *et al.*, 2008) that in early embryos, at least, MP is still expressed in *obe1 obe2* mutants. It is therefore possible that OBE functions downstream of MP in embryos (Saiga *et al.*, 2008). For MP to function as an ARF, auxin-mediated decay of BDL must release MP from the ARF-Aux/IAA complex. Hence, we determined whether the SCF decay pathway for Aux/IAA proteins is functional in *obe1-1 obe2-2* mutant seedlings. The *HSp:NTAXR3.GUS* construct provides an effective reporter of degradation of auxin-induced Aux/IAA (AXR3 in this case) (Gray *et al.*, 2001). As a control we used *HSp:GUS*. Both constructs were transformed into *obe1-1/obe1-1 OBE2/obe2-2* plants, and lines homozygous for the reporter constructs were selected. Mutant *obe1-1 obe2-2* seedlings carrying *HSp:NTAXR3.GUS* were compared with mutant seedlings carrying *HSp:GUS* for stability of heat shock-induced GUS expression in the absence and presence of exogenously added auxin. Similar experiments have previously examined GUS activity in excised roots (Gray *et al.*, 2001). This was not possible for *obe1-1 obe2-2* double mutants, so comparisons were made for GUS activity in intact mutant seedlings. Addition of auxin after heat-shock treatment for 2 h showed no change in control tissues (GUS alone, Figure 6c,d), but resulted in increased degradation of AXR3.GUS in mutant seedlings (Figure 6a,b), indicating that the SCF^{TIR1} pathway is functional in *obe1-1 obe 2-2* double mutants.

Auxin gradients are correctly established in *obe1 obe2* mutant embryos

Failure of *mpG12* and *bdl* mutants to specify the primary root meristem and vascular initials in embryos is associated with an inability of mutant tissues to form relevant auxin maxima (Weijers *et al.*, 2006). As OBE proteins appear to function downstream of MP and auxin-directed degradation of Aux/IAA proteins operates correctly in *obe1-1 obe2-2* double mutants, we predicted that, unlike the situation in *mpG12* and *bdl* mutants, embryonic auxin maxima would be formed in *obe1-1 obe2-2* mutants. The *pDR5rev:GFP* reporter of cellular auxin signalling is thought to reflect endogenous auxin response maxima (Benkova *et al.*, 2003). Segregating mutant and wild-type siblings carrying the

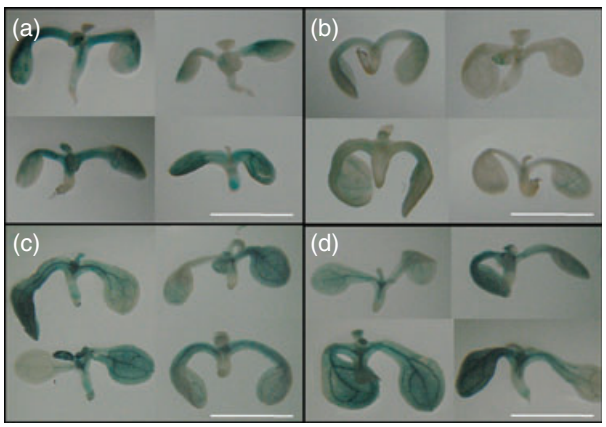

Figure 6. Analysis of the SCF decay pathway in *obe1-1 obe2-2* seedlings. Seven-day-old *obe1-1 obe2-2 HSp:NTAXR3GUS* (a, b) and *obe1-1 obe2-2 HSp:GUS* (c, d) seedlings were heat-shocked and treated with naphthalene acetic acid (b, d) or left untreated (a, c) and stained for GUS activity. Scale bar = 0.25 cm.

homozygous reporter were analysed for GFP fluorescence in developing embryos using confocal laser scanning microscopy (Figure 7).

Embryos from selfed lines of *OBE1/obe1-1 obe2-2/obe2-2* (or the reciprocal) nearly all showed a pattern of GFP fluorescence in early embryos similar to that described previously (Friml *et al.*, 2003) for wild-type embryos. Briefly, immediately after the first zygotic division, fluorescence became concentrated in the apical tissues with little fluorescence in the suspensor. Around the 32-cell stage, the apical–basal gradient becomes reversed, as most *pDR5rev* activity is shifted towards basal cells including the uppermost suspensor cell and the hypophysis. In approximately 25% of embryos, taken to be mutants, a subtly different series of events occurred. These included higher levels of GFP fluorescence, representing an increase in the overall auxin response maximum. Hence, early globular (16-cell) stage embryos (9/33) showed fluorescence being retained within the suspensor, whereas this was lost for the majority of

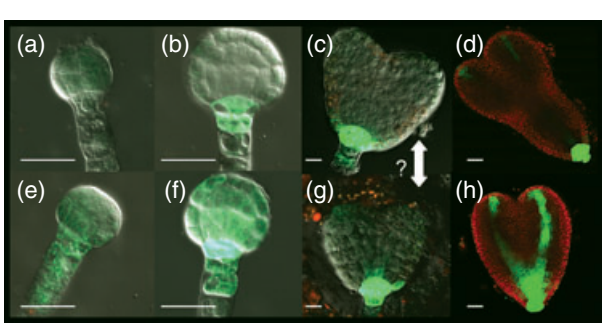

Figure 7. *pDR5rev:GFP* reporter activity in *obe1-1 obe2-2* embryos. Embryos were dissected from segregating *obe1-1/obe1-1 OBE2/obe2-2 pDR5rev:GFP* homozygous lines and analysed for GFP expression by confocal laser scanning microscopy. Wild-type embryos (a, b, d) and *obe1-1 obe2-2* embryos (e, f, h). In heart stage embryos, the GFP phenotype was indistinguishable between mutant and wild-type (c, g). Scale bars = 20 μm.

embryos (wild-type) at this stage (Figure 7a,b,e). At the globular stage, when the auxin response maximum was strongly focused at the hypophysis in wild-type embryos, a minority (19/45) of sibling embryos also showed a strong auxin response maximum at the hypophysis, but this was less well focused (Figure 7b,f). In putative mutant embryos the position of the auxin response maximum continued to be focused to the root pole, such that, at heart stage, mutant and wild-type embryos were indistinguishable (Figure 7c,g).

Later in development (torpedo stage), fluorescence maxima in embryos from wild-type plants were located within the QC and at the tips of developing cotyledons, with faint fluorescence along the anticipated vascular path for hypocotyls and the central cotyledonary veins. For the segregating mutant line, two types of pattern were again visible. The majority (21/35) of embryos showed wild-type patterns of *pDR5rev:GFP* response. In contrast, 14/35 showed much stronger fluorescence with maxima at the putative root tip and tips of the cotyledons, and with the location of potential vascular paths very clearly defined as strong GFP fluorescence in the hypocotyl and cotyledons (Figure 7d,e). This pattern of fluorescence was very similar to the consequences of exogenous auxin treatment of torpedo stage embryos (Friml *et al.*, 2003). These results show that, as predicted, the auxin response maxima at the root pole and along the vascular path are established in the *obe1-1 obe2-2* double mutant.

Redundant OBE functions correlate with protein–protein interactions

Our data, and previous data (Saiga *et al.*, 2008), show that *OBE1* and *OBE2* encode redundant functions. One scenario for such redundancy is that the OBE proteins physically interact with each other. To test this, we subjected OBE proteins to a two-hybrid protein interaction assay in yeast. Arabidopsis encodes four related PHD finger domain proteins [OBE1, OBE2, OBE3, OBE4] that form two distinct sub-clades (Saiga *et al.*, 2008). The four OBE proteins were tested for their ability to interact with each other and with themselves (Figure S2). All four OBE proteins interacted with OBE1 and OBE2. In addition, OBE1 and OBE2, but not OBE3 and OBE4, were able to self-interact, and OBE3 and OBE4 did not interact with each other. Hence, there is potential for OBE1 and OBE2 to work in concert with each other in complexes involving homo- and hetero- interactions.

DISCUSSION

Plant hormones are intimately involved in controlling the location and timing of tissue patterning in embryos. Although *obe1 obe2* double mutant phenotypes were visible in germinated seedlings, most of the defects were established during embryo development. This was especially true for root and vascular phenotypes; mutant seedlings showed

true leaves but these failed to develop further (Saiga *et al.*, 2008). The correlation of pleiotropic phenotypes in *obe1 obe2* mutants with those for the *mpG12* mutant suggested a link with auxin signalling. This was supported by the abundance of auxin-related functions in lists of genes showing significantly altered regulation in mutant seedlings and RNAi plants, and genetic relationships revealed in crosses with *pin1-7*, *mpG12* and *bdl*.

Auxin mediates developmental patterning through a complex network of functions that include the PIN influx proteins, Aux/IAA receptors, ARF transcription factors and reinforcing transcriptional feedback loops. In embryonic patterning of roots, formation of an auxin maximum in the hypophysis directs the asymmetric division required to establish the progenitors of the QC and columella. With respect to OBE function, Saiga *et al.* (2008) suggested that the expression of *MP* in *obe1 obe2* double mutant embryos indicates that OBE proteins operate downstream of MP/BDL to mediate establishment of the root apical meristem. They also showed that *obe1 obe2* double mutants fail to express *PLETHORA* (*PLT*), *SCARECROW* (*SCR*) or *WOX5*, in line with the absence of QC specification. We broadly agree with this conclusion, and have further shown that *OBE* expression is not under the direct control of MP ARF activity. Also, the SCF^{TIR1} pathway is unaffected, making it likely that auxin is correctly sensed and that stimulated dissociation of BDL from MP occurs. More significantly, we predicted that the *obe1 obe2* mutant would still be able to form an auxin maximum at the root pole. Mutations in *MP* and *BDL* prevent formation of the auxin maximum in the hypophysis and formation of the QC (Weijers *et al.*, 2006). *PIN1* mutants still form roots (and presumably still exhibit an auxin maximum at the hypophysis during early development). In contrast, using the *pDR5rev:GFP* reporter, we showed that *obe1 obe2* double mutants retained the ability to form an auxin-response maximum, and in doing so must have functional PIN activity. Although mutant embryos also accumulated an apparently higher level of auxin, this did not prevent formation of an auxin maximum at the hypophysis appropriate for auxin-directed asymmetric division to define the QC. However, embryos with a higher level of auxin appeared to take longer to achieve a strongly focused maximum at the hypophysis. It is not clear whether it is absolute or relative accumulation of auxin at the hypophysis that is critical in triggering the asymmetric division. If the latter, then higher auxin accumulation may have led to a relative delay in achieving an auxin maximum at a critical stage in embryo development. Nevertheless, our data suggest that OBE function operates at a point in auxin-induced transcriptional activation beyond accumulation and sensing of auxin.

The uniform expression of *OBE1* and *OBE2* during early stages of embryo development correlates with the position and timing for correct hypophyseal divisions and QC specification. *OBE1* and *OBE2* are also expressed throughout torpedo and early cotyledonary stage embryos, although transcriptional activity is concentrated at the root pole. Hence, they are also correctly positioned for establishment of the early vascular system.

OBE genes continue to be expressed in growing seedling roots, and, indeed, throughout most of the adult plant. Any later phenotypes resulting as a consequence of *OBE* mutations would have been obscured because of the strong embryo phenotype and would probably only be revealed through use of weak *obe* alleles. More research is necessary to determine whether such additional roles differ from those in the embryo, but our preliminary transcript profiling data indicate, for example, reduced expression of *MP* in seedling aerial tissues inconsistent with preserved *MP* expression in the developing embryo (Saiga *et al.*, 2008).

In older mutant embryos, the *pDR5rev:GFP* reporter identified predicted paths for vasculature in the hypocotyl and the primary vein in developing cotyledons, even though no vasculature developed in the former and only an incomplete network was present in the seedling cotyledons. MP is also implicated as a central factor in vascular development (Hardtke and Berleth, 1998). This connection with MP fits with our analyses based upon genetic interactions. Hence synergistic interactions with *BDL* and *PIN1* indicate overlapping rather than epistatic relationships, whereas there was a closer relationship with *MP*, with phenotypes of triple *obe 1-1 obe2-2 mpG12* mutants that were similar to, but at the more extreme end of the scale of *mpG12* phenotypes. This indicates that *MP* is epistatic to *OBE* genes, although MP may not directly regulate *OBE* expression as this is not affected in *mpG12* mutants.

Embryonic patterning of the root and vasculature is one of the best understood of the auxin-directed developmental pathways. A large number of genes and processes have been implicated. These include the central roles played by MP and BDL in acting non-cell autonomously to specify the primary root meristem and procambial tissues. Many additional downstream steps have been identified, including PLT, SCR and WOX5. With the exception of TOPLESS, which participates in chromatin-mediated transcriptional repression to establish the embryonic polar axis (Long *et al.*, 2006), there has been little evidence for chromatin-mediated auxin-triggered regulation of tissue patterning. As PHD finger domain proteins, OBE1 and OBE2 define an additional layer of transcriptional control, potentially acting through recognition of the methylation status of lysine 4 on chromatin histone H3 in the transduction of auxin accumulation into transcriptional outputs for specification of root meristem and vasculature in the embryo. Saiga *et al.* (2008) propose that these proteins act to establish and/or maintain both the shoot and root meristems. Our data are consistent with this broad conclusion, although partial development of the shoot organs in the *obe1 obe2* mutant indicates that

the shoot phenotype is a lesser or indirect effect when compared to interference in the MP pathway, including complete failure of the root meristem and defective development of a contiguous vasculature.

Phenotypic similarity with mutants in major auxin-regulated genes, particularly for the vasculature and root meristem, and genetic overlap with other auxin-related genes, suggest that *OBE1* and *OBE2* act redundantly in the regulation of auxin functions. Widespread expression of these genes indicates wider roles in growth and development. As OBE1 and OBE2 form half of a larger family of related and interacting PHD finger domain proteins, it will be interesting also to uncover the phenotypic and functional consequences of mutations in *At1g14740* (*OBE3*) and *At3g63500* (*OBE4*).

The emerging picture for OBE functions is that they represent a second level of control in the auxin-signalling pathway. Our genetic data suggest that this control is connected to the canonical auxin-signalling pathway via PINs, ARFs and AUX/IAA intermediaries. However, we cannot exclude the possibility that OBE proteins operate within the context of a parallel pathway. The widespread expression of *OBE1* and *OBE2*, not restricted in space or time to the occurrence of auxin maxima, suggest that they could provide a regulatory platform for the translation of auxin signals into functional outputs, most likely through the modification of chromatin.

EXPERIMENTAL PROCEDURES

Plant materials

Arabidopsis thaliana Columbia (Col-0) T-DNA insertion mutants *obe1-1* (SALK_075710), *pin1-7* (SALK_047613) and the *A. thaliana* Landsberg *erecta* (L*er*) *obe2-2* TILLING mutant (CS94914) were obtained from the Arabidopsis Biological Resource Center (ABRC). Lines *mp12G*, *bdl*, *HSp:NTAXR3.GUS* and *HSp:GUS*, and *pDR5rev:GFP* were kindly provided by Thomas Berleth (Cell and Systems Biology, University of Toronto), Gerd Jürgens (Centre for Plant Molecular Biology, University of Tubingen), Ottoline Leyser (Department of Biology, University of York) and Jiri Friml (Department of Plant Biotechnology and Genetics, University of Ghent), respectively. OBE mutants were propagated as either *OBE1-1/obe1-1 obe2-2/obe2-2* or *obe1-1/obe1-1 OBE2-2/obe2-2* lines. Plants were grown under long-day conditions (18 h photoperiod, 22°C).

Yeast two-hybrid analysis

Yeast two-hybrid analysis was performed using the Matchmaker GAL4 two-hybrid system (Clontech, http://www.clontech.com/) as described by the manufacturer. Bait constructs containing coding sequences for *OBE1* (*At3g07780*), *OBE2* (*At5g48160*) and the related sequences *At1g14740* (*OBE3*) and *At3g63500* (*OBE4*) were amplified from a pool of Arabidopsis Col-0 cDNA, cloned into *pGBT9*, and transformed into yeast strain CG1945. Prey constructs of the same genes were cloned into *pGAD424* and transformed into yeast strain Y187. Protein–protein interactions were identified by yeast mating experiments, and from the ability of co-transformed yeast to grow on synthetic medium lacking leucine, tryptophan and histidine and containing 5 mM 3-aminotriazole. A human lamin binding domain fusion was used as a negative control to assess extraneous interaction of the binding domain with the prey.

Construction of plasmids and transgenic plants

Gateway™ technology (Invitrogen, http://www.invitrogen.com/) was used to generate all clones in this publication. Primer sequences used for cloning are available upon request. Gene sequences were amplified by PCR using Phusion DNA polymerase (NEB, http://www.neb.com). Resulting DNA fragments were purified and transferred by recombination into the entry vector pDONR207 (Invitrogen) using BP clonase II (Invitrogen), and the sequence of the resulting pDONR clone was verified. Transfer to the indicated binary destination vector using LR clonase II (Invitrogen) was performed as described by the manufacturer. Reporter plasmids expressing *GFP.GUS* or *nlsGFP* from *OBE1p* and *OBE2p* promoters were constructed by recombining a 1 kb genomic sequence immediately upstream of the ATG of *OBE1* and *OBE2*, amplified by PCR, into pDONR207. After sequence verification, fragments were transferred into the destination vector pB7GWFS (Karimi *et al.*, 2005) to give *OBEp:GFP.GUS*. Alternatively, the same promoter fragments were amplified using overlap PCR to add an SV40 NLS to the N-terminus of GFP, to generate *OBE:pnlsGFP*. This was recombined into pDONR207 before transfer into the binary destination vector pEARLEYGATE301 (Earley *et al.*, 2006), resulting in reporter plasmids *OBE1p:nlsGFP* and *OBE2p:nlsGFP*. For mutant complementation, *OBE1p:OBE1.GFP*, *OBE2p:OBE2.HA*, *35Sp:OBE1*, *35Sp:OBE2*, *AtRPS5Ap:OBE1* and *AtRPS5Ap:OBE2* plasmids were constructed. *OBE1p:OBE1* and *OBE2p:OBE2* genomic fragments, starting 1 kb upstream of the ATG and ending immediately before the termination codon, were used in overlap PCR reactions to generate a fusion with GFP or a haemagglutinin tag, respectively. *OBE* coding sequences were either fused by overlap PCR to a 1.7 kb genomic fragment containing the promoter region of *AtRPS5A* to create *AtRPS5Ap:OBE1* and *AtRPS5Ap:OBE2* fusions, or used directly for recombination into pDONR207 before transfer into either binary destination vector pEARLEYGATE301 (Earley *et al.*, 2006), resulting in *OBE1p:OBE1.GFP*, *OBE2p:OBE2.HA*, *AtRPS5Ap:OBE1* and *AtRPS5Ap:OBE2*, or binary destination vector pB7GW2.0 (Karimi *et al.*, 2005) to generate *35Sp:OBE1* and *35Sp:OBE2*. All constructs were transformed into *Agrobacterium tumefaciens* strain GV3101 by electroporation, and used to transform Arabidopsis using the floral dip method (Clough and Brent, 1998). The reporter constructs *OBE1p:GFP.GUS* and *OBE2p:GFP.GUS* were transformed into wild-type Arabidopsis Col-0, whereas *OBE1p:OBE1.GFP*, *35Sp:OBE1* and *AtRPS5Ap:OBE1* were transformed into *obe1-1/obe1-1 OBE2/obe2-2* lines, and *OBEp:OBE2.HA*, *35SpOBE2* and *35SAtRPS5Ap:OBE2* were transformed into *OBE1/obe1-1 obe2-2/obe2-2* lines.

Genotypic analysis

For triple mutant analysis, genomic DNA was isolated from Arabidopsis grown on MS plates and genotyped for the presence of *obe1-1*, *obe2-2*, *mpG12*, *bdl* or *pin1-7* or their wild-type alleles. The genotype at the *OBE1* locus was identified by the presence of a specific band of 1 kb when using OBE1FW and OBE1RV primers and the absence of a T-DNA insertion band of 1.2 kb when using LBa1 and OBE1RV2 primers. The *obe2-2* allele was identified by the presence of a specific band of 1.2 kb when using OBE2FW and OBE2RV primers, followed by a diagnostic *Mly*I digest. The genotype at the *BDL* locus was identified by PCR amplification of an 800 bp *BDL* fragment when using BDLFW and BDLRV primers, followed by a diagnostic *Hae*III digest. Genotyping at the *MP* locus was marked by the presence of a 2.6 kb band when using BS1354-f

and BS1354-r primers. The genotype of *PIN1* was determined by the presence of a gene-specific fragment of 988 bp when using PIN1LP and PIN1RP primers, and the absence of a 500 bp T-DNA specific fragment when using primers PIN1RP and LBb1. Primer sequences are available on request.

Phenotypic analysis

Sterilized seeds were sown on MS plates and incubated in the dark at 4°C for 48 h before being transferred to a growth room. Seedling phenotypes were assessed after 3 weeks; seedlings were observed and photographed under a dissecting microscope (Zeiss StemiSV11, http://www.zeiss.com/). For crosses between *obe1-1 obe2-2* and *mpG12*, rootless progeny were phenotyped using an arbitrary scale (1–4) where 1 = seedlings with two equal cotyledons, 2 = seedlings with one larger cotyledon, 3 = seedlings with a single cotyledon and vestigial leaves at the apex, and 4 = seedlings with a single cotyledon and no visible leaves. Each seedling was genotyped.

To analyse the vein patterning in mutant and wild-type seedlings, seedlings were fixed in a 6:3:1 mixture of ethanol:acetic acid:water overnight, chlorophyll was removed using 100% and 70% v/v ethanol, and the tissue was cleared by overnight incubation in Hoyer's reagent (Meinke, 1994).

For embryos, siliques of soil-grown *obe1-1/obe1-1 OBE2/obe2-2* or *OBE1/obe1-1 obe2-2/obe2-2* lines were sliced open under a dissecting microscope and ovules were cleared using Hoyer's solution. Embryos were observed by differential interference contrast (DIC) microscopy using a confocal laser scanning microscope (Zeiss 510 meta-analyzer). Reporter lines *OBE1p:GFP.GUS*, *OBE2p:GFP.GUS*, *OBE1p:nlsGFP* and *OBE2p:nlsGFP* were used to investigate tissue-specific expression in embryos and roots. Embryos were dissected directly into MS medium; for roots, seedlings were grown on vertical MS plates. Using a confocal laser scanning microscope, GFP was excited at 488 nm and emitted light captured at 505–555 nm; light emitted at 630–680 nm showed chlorophyll autofluorescence. It was not possible to establish cellular patterning phenotypes from dissected embryos used for fluorescence microscopy without fixation. GUS activity in transgenic wild-type seedlings either untreated or treated with 5 nM naphthalene acetic acid was determined as described by Saiga *et al.* (2008).

For testing the activity of the SCF^{TIR1} pathway, 7-day-old *HSp:GUS* or *HSp:NTAXR3.GUS* homozygous seedlings, also segregating for the *obe1-1/obe1-1 OBE2/obe2-2* mutant genotype, were heat-shocked for 2 h at 37°C in MS medium. After transfer to room temperature for 20 min, seedlings were stained for GUS activity as above.

Expression analysis

For microarray analysis of RNAi lines, aerial tissues of 5-week-old plants were harvested for RNA extraction. Three biological replicates per line were used. Each replicate consisted of pools of three or four (Col-0) or six to eight (*obe1i obe2i* line) individual plants. For microarray analysis of the *obe1-1 obe2-2* double mutant, segregating seedlings (pools of 15–20 seedlings; three biological replicates) from the *obe1-1/obe1-1 OBE2/obe2-2* selfed line were grown for 12 days on agar plates before being harvested. Rootless mutant seedlings were compared with wild-type siblings from which roots had been removed; in parallel, the mutant seedlings were wounded at the bottom of their vestigial hypocotyl. Total RNA was extracted using TRI reagent (Sigma, http://www.sigmaaldrich.com/) and further purified using RNeasy mini-columns (Qiagen, http://www.qiagen.com/). ATH1 Arabidopsis genome arrays (Affymetrix) were hybridized by the Nottingham Arabidopsis Stock Centre International Affymetrix Service (http://affymetrix.arabidopsis.info) or the John Innes Centre Genome Laboratory Affymetrix Service (http://jicgenomelab.co.uk/microarrays) using the methods described by the GENECHIP® Expression Analysis Technical Manual (http://www.affymetrix.com/support/technical/manuals.affx).

Statistical analysis was performed using the open source software project Bioconductor (Gentleman *et al.*, 2004). Raw data were normalized using the robust multichip average (RMA) function implemented in the *affy* package (Gautier *et al.*, 2004). This function background-corrects perfect-match values using the non-linear RMA method, normalizes them using quantile normalization, and finally summarizes them to give a set of $\log_2$-transformed expression measures. As such, this function provides better precision, more consistent estimates of fold change, and higher specificity and sensitivity than other methods when using fold change analysis to detect differential expression (Irizarry *et al.*, 2003). Comparisons between treated plants and their controls were performed using the *limma* package (Smyth, 2005). Differentially expressed genes were identified using two filters: a false discovery rate-corrected *t* test (*P* value cut-off set at 0.05) (Reiner *et al.*, 2003) and $\log_2$ of fold change [log(FC)] >1 or <−1. Data are publicly available from the Gene Expression Omnibus (http://www.ncbi.nlm.nih.gov/geo/index.cgi), with accession number GSE10248.

Quantitative real-time RT-PCR

Quantitative real-time RT-PCR was performed on selected genes using standard SYBR Green assays (SYBR® Green JumpStart™ *Taq* ReadyMix™; Sigma) on a DNA Engine Opticon 2 machine (Bio-Rad, http://www.bio-rad.com/). Primer sequences for *ARF1*, *ARF2*, *ARF5/MP*, *ARF10*, *ARF11*, *IAA12/BDL*, *IAA14*, *AXR3/IAA17* and *IAA32* are available in Czechowski *et al.* (2004), those for *PID* in Lee and Cho (2006), and those for *PIN1* in Peer *et al.* (2004). Primers OBE1FW3/OBER3 and OBE2FW2/OBE2R2 were used for quantitative real-time RT-PCR of *OBE1* and *OBE2* RNAs, respectively. Expression of *OBE* genes in *mpG12* whole mutant seedlings was assessed by semi-quantitative PCR.

ACKNOWLEDGEMENTS

We thank Liam Dolan and Robert Sablowski for valuable discussions and for critically reviewing the work prior to submission. We also thank Thomas Berleth (Cell and Systems Biology, University of Toronto), Gerd Jürgens (Centre for Plant Molecular Biology, University of Tubingen), Ottoline Leyser (Department of Biology, University of York) and Jiri Friml (Department of Plant Biotechnology and Genetics, University of Ghent) for providing biological materials. C.L.T. and D.S. were funded (BBS/B/0658X), and the John Innes Centre was grant-aided, by the UK Biotechnology and Biological Sciences Research Council.

SUPPORTING INFORMATION

Additional Supporting Information may be found in the online version of this article:

Figure S1. Overlap in altered RNA profiles between *obe1-1 obe2-2* and *obe1i obe2i* seedlings.

Figure S2. Yeast two-hybrid assay of the interaction between OBE proteins.

Table S1. Genes differentially expressed in the *obe1-1 obe2-2* double mutant when compared to wild-type.

Table S2. Genes differentially expressed in the *obe1i obe2i* mutant seedlings when compared to wild-type.

Table S3. Changes in auxin-related genes are over-represented in *obe1 obe 2* mutants.

Table S4. Relative expression of auxin-related genes.

Table S5. Microarray data for genes encoding proteins involved in the auxin biosynthesis pathway.

REFERENCES

Benkova, E., Michniewicz, M., Sauer, M., Teichmann, T., Seifertova, D., Jürgens, G. and Friml, J. (2003) Local, efflux-dependent auxin gradients as a common module for plant organ formation. *Cell*, **115**, 591–602.

Berleth, T. and Jürgens, G. (1993) The role of the *MONOPTEROS* gene in organizing the basal body region of the *Arabidopsis* embryo. *Development*, **118**, 575–587.

Berleth, T., Mattsson, J. and Hardtke, C.S. (2000) Vascular continuity and auxin signals. *Trends Plant Sci.* **5**, 387–393.

Blakeslee, J.J., Peer, W.A. and Murphy, A.S. (2005) Auxin transport. *Curr. Opin. Plant Biol.* **8**, 494–500.

Clough, S.J. and Bent, A.F. (1998) Floral dip: a simplified method for *Agrobacterium tumefaciens* mediated transformation of *Arabidopsis thaliana*. *Plant J.* **16**, 735–743.

Cosgrove, M.S. (2006) PHinDing a new histone 'effector' domain. *Structure*, **14**, 1096–1098.

Czechowski, T., Bari, R.P., Stitt, M., Scheible, W.R. and Udvardi, M.K. (2004) Real-time RT-PCR profiling of over 1400 Arabidopsis transcription factors: unprecedented sensitivity reveals novel root- and shoot-specific genes. *Plant J.* **38**, 366–379.

De Smet, I. and Jürgens, G. (2007) Patterning the axis in plants – auxin in control. *Curr. Opin. Genet. Dev.* **17**, 337–343.

Dharmasiri, N., Dharmasiri, S. and Estelle, M. (2005) The F-box protein TIR1 is an auxin receptor. *Nature*, **435**, 441–445.

Dunoyer, P., Thomas, C., Harrison, S., Revers, F. and Maule, A. (2004) A cysteine-rich plant protein potentiates Potyvirus movement through an interaction with the virus genome-linked protein VPg. *J. Virol.* **78**, 2301–2309.

Earley, K.W., Haag, J.R., Pontes, O., Opper, K., Juehne, T., Song, K. and Pikaard, C.S. (2006) Gateway-compatible vectors for plant functional genomics and proteomics. *Plant J.* **45**, 616–629.

Friml, J., Vieten, A., Sauer, M., Weijers, D., Schwarz, H., Hamann, T., Offringa, R. and Jürgens, G. (2003) Efflux-dependent auxin gradients establish the apical–basal axis of Arabidopsis. *Nature*, **426**, 147–153.

Galweiler, L., Guan, C., Muller, A., Wisman, E., Mendgen, K., Yephremov, A. and Palme, K. (1998) Regulation of polar auxin transport by AtPIN1 in Arabidopsis vascular tissue. *Science*, **282**, 2226–2230.

Gautier, L., Cope, L., Bolstad, B.M. and Irizarry, R.A. (2004) affy – analysis of *Affymetrix GeneChip* data at the probe level. *Bioinformatics*, **20**, 307–315.

Gentleman, R.C., Carey, V.J., Bates, D.M. *et al.* (2004) Bioconductor: open software development for computational biology and bioinformatics. *Genome Biol.* **5**, R80.

Gray, W.M., Kepinski, S., Rouse, D., Leyser, O. and Estelle, M. (2001) Auxin regulates SCFTIR1-dependent degradation of AUX/IAA proteins. *Nature*, **414**, 271–276.

Hamann, T., Mayer, U. and Jürgens, G. (1999) The auxin-insensitive *bodenlos* mutation affects primary root formation and apical–basal patterning in the Arabidopsis embryo. *Development*, **126**, 1387–1395.

Hamann, T., Benkova, E., Baurle, I., Kientz, M. and Jürgens, G. (2002) The Arabidopsis BODENLOS gene encodes an auxin response protein inhibiting MONOPTEROS-mediated embryo patterning. *Genes Dev.* **16**, 1610–1615.

Hardtke, C.S. and Berleth, T. (1998) The *Arabidopsis* gene *MONOPTEROS* encodes a transcription factor mediating embryo axis formation and vascular development. *EMBO J.* **17**, 1405–1411.

Hardtke, C.S., Ckurshumova, W., Vidaurre, D.P., Singh, S.A., Stamatiou, G., Tiwari, S.B., Hagen, G., Guilfoyle, T.J. and Berleth, T. (2004) Overlapping and non-redundant functions of the *Arabidopsis* auxin response factors *MONOPTEROS* and *NONPHOTOTROPIC HYPOCOTYL 4*. *Development*, **131**, 1089–1100.

Irizarry, R.A., Bolstad, B.M., Collin, F., Cope, L.M., Hobbs, B. and Speed, T.P. (2003) Summaries of Affymetrix GeneChip probe level data. *Nucleic Acids Res.* **31**, e15.

Jenik, P.D., Gillmor, C.S. and Lukowitz, W. (2007) Embryonic patterning in *Arabidopsis thaliana*. *Annu. Rev. Cell Dev. Biol.* **23**, 207–236.

Karimi, M., De Meyer, B. and Hilson, P. (2005) Modular cloning in plant cells. *Trends Plant Sci.* **10**, 103–105.

Kramer, E.M. and Bennett, M.J. (2006) Auxin transport: a field in flux. *Trends Plant Sci.* **11**, 382–386.

Lee, S.H. and Cho, H.T. (2006) PINOID positively regulates auxin efflux in *Arabidopsis* root hair cells and tobacco cells. *Plant Cell*, **18**, 1604–1616.

Leyser, O. (2006) Dynamic integration of auxin transport and signalling. *Curr. Biol.* **16**, R424–R433.

Long, J.A., Ohno, C., Smith, Z.R. and Meyerowitz, E.M. (2006) TOPLESS regulates apical embryonic fate in *Arabidopsis*. *Science*, **312**, 1520–1522.

Martin, D.G.E., Baetz, K., Shi, X.B., Walter, K.L., MacDonald, V.E., Wlodarski, M.J., Gozani, O., Hieter, P. and Howe, L. (2006) The Yng1p plant homeodomain finger is a methyl-histone binding module that recognizes lysine 4-methylated histone H3. *Mol. Cell. Biol.* **26**, 7871–7879.

Meinke, D.W. (1994) Seed development in *Arabidopsis*. In *Arabidopsis* (Meyerowitz, E.M. and Somerville, C.R., eds). Cold Spring Harbor, NY: Cold Spring Harbor Laboratory Press, pp. 253–295.

Peer, W.A., Bandyopadhyay, A., Blakeslee, J.J., Makam, S.N., Chen, R.J., Masson, P.H. and Murphy, A.S. (2004) Variation in expression and protein localization of the PIN family of auxin efflux facilitator proteins in flavonoid mutants with altered auxin transport in *Arabidopsis thaliana*. *Plant Cell*, **16**, 1898–1911.

Peña, P.V., Davrazou, F., Shi, X.B., Walter, K.L., Verkhusha, V.V., Gozani, O., Zhao, R. and Kutateladze, T.G. (2006) Molecular mechanism of histone H3K4me3 recognition by plant homeodomain of ING2. *Nature*, **442**, 100–103.

Ramon-Maiques, S., Kuo, A.J., Carney, D., Matthews, A.G.W., Oettinger, M.A., Gozani, O. and Yang, W. (2007) The plant homeodomain finger of RAG2 recognizes histone H3 methylated at both lysine-4 and arginine-2. *Proc. Natl Acad. Sci. USA*, **104**, 18993–18998.

Reiner, A., Yekutieli, D. and Benjamini, Y. (2003) Identifying differentially expressed genes using false discovery rate controlling procedures. *Bioinformatics*, **19**, 368–375.

Saiga, S., Furumizu, C., Yokoyama, R., Kurata, T., Sato, S., Kato, T., Tabata, S., Suzuki, M. and Komeda, Y. (2008) The *Arabidopsis OBERON1* and *OBERON2* genes encode plant homeodomain finger proteins and are required for apical meristem maintenance. *Development*, **135**, 1751–1759.

Scarpella, E., Marcos, D., Friml, J. and Berleth, T. (2006) Control of leaf vascular patterning by polar auxin transport. *Genes Dev.* **20**, 1015–1027.

Smyth, G.K. (2005) Limma: linear models for microarray data. In *Bioinformatics and Computational Biology Solutions using R and Bioconductor* (Gentleman, R., Carey, V., Dudoit, S., Irizarry, R. and Huber, W., eds). New York: Springer, pp. 397–420.

Sunilkumar, G., Mohr, L., Lopata-Finch, E., Emani, C. and Rathore, K.S. (2002) Developmental and tissue-specific expression of CaMV 35S promoter in cotton as revealed by GFP. *Plant Mol. Biol.* **50**, 463–474.

Tan, X., Calderon-Villalobos, L.I.A., Sharon, M., Zheng, C., Robinson, C.V., Estelle, M. and Zheng, N. (2007) Mechanism of auxin perception by the TIR1 ubiquitin ligase. *Nature*, **446**, 640–645.

Vieten, A., Vanneste, S., Wisniewska, J., Benkova, E., Benjamins, R., Beeckman, T., Luschnig, C. and Friml, J. (2005) Functional redundancy of PIN proteins is accompanied by auxin-dependent cross-regulation of *PIN* expression. *Development*, **132**, 4521–4531.

Weijers, D. and Jürgens, G. (2005) Auxin and embryo axis formation: the ends in sight? *Curr. Opin. Plant Biol.* **8**, 32–37.

Weijers, D., Franke-van Dijk, M., Vencken, R.J., Quint, A., Hooykaas, P. and Offringa, R. (2001) An *Arabidopsis* Minute-like phenotype caused by a semi-dominant mutation in a *RIBOSOMAL PROTEIN S5* gene. *Development*, **128**, 4289–4299.

Weijers, D., Benkova, E., Jäger, K.E., Schlereth, A., Hamann, T., Kientz, M., Wilmoth, J.C., Reed, J.W. and Jürgens, G. (2005) Development specificity of auxin response by pairs of ARF and AUX/IAA transcriptional regulators. *EMBO J.* **24**, 1874–1885.

Weijers, D., Schlereth, A., Ehrismann, J.S., Schwank, G., Kientz, M. and Jürgens, G. (2006) Auxin triggers transient local signaling for cell specification in Arabidopsis embryogenesis. *Dev. Cell*, **10**, 265–270.

Wisniewska, J., Xu, J., Seifertova, D., Brewer, P.B., Ruzicka, K., Blilou, I., Rouquie, D., Scheres, B. and Friml, J. (2006) Polar PIN localization directs auxin flow in plants. *Science*, **312**, 883.

Yang, Y.D., Hammes, U.Z., Taylor, C.G., Schachtman, D.P. and Nielsen, E. (2006) High-affinity auxin transport by the AUX1 influx carrier protein. *Curr. Biol.* **16**, 1123–1127.

